

## SUPERCONDUCTING BOOSTER CYCLOTRON STUDIES AT GANIL.

A. Chabert, C. Bieth, P. Bricault, M. Duval, J. Fermé, A. Joubert, M.H. Moscatello, F. Ripouteau, Q.V. Truong.

GANIL - B.P. 5027 - F-14021 Caen Cedex.

**Abstract :** The study of a booster cyclotron SSC3 giving a maximum energy around 500 MeV/A for light ions has been performed at GANIL. SSC3 is a separated sector cyclotron using separated superconducting coils. The results concerning these studies are reported.

**Introduction :** The GANIL facility provides ions from C to U at maximum energies and intensities ranging from 100 MeV/A,  $10^{13}$  pps for light ions, down to 25 MeV/A,  $10^{10}$  pps for the heaviest ones. Among various possible developments of our laboratory, it would be very fascinating to increase the maximum energy in the 500 MeV/A range while preserving the beam intensities and still improving its qualities. A new separated sector cyclotron is the booster suited to this goal.

### I. Main parameters and description of SSC3.

The mean ejection radius ( $\bar{r}_{out} = 3\text{m}$ ) and the RF frequency range ( $f = 7 - 13.36\text{ MHz}$ , 2<sup>nd</sup> harmonic) of SSC2 being given, it turns out that the ratio of SSC3 ejection to injection radii has to be larger than 1.8 in order to reach 500 MeV/A. We have chosen  $\bar{r}_{out} = 2 \bar{r}_{in}$  and restricted the SSC2 frequency range to 7 - 12 MHz when injecting into SSC3. The SSC3 maximum energy will then be 490 MeV/A and will be reached at  $\bar{B} \cdot r = 7.144\text{ Tm}$  for ions of  $Q/A = 0.5$ , we will also limit the maximum SSC3 rigidity to this value.

From these choices, we deduce the SSC3 energy range versus  $Q/A$  as shown on figure 1.

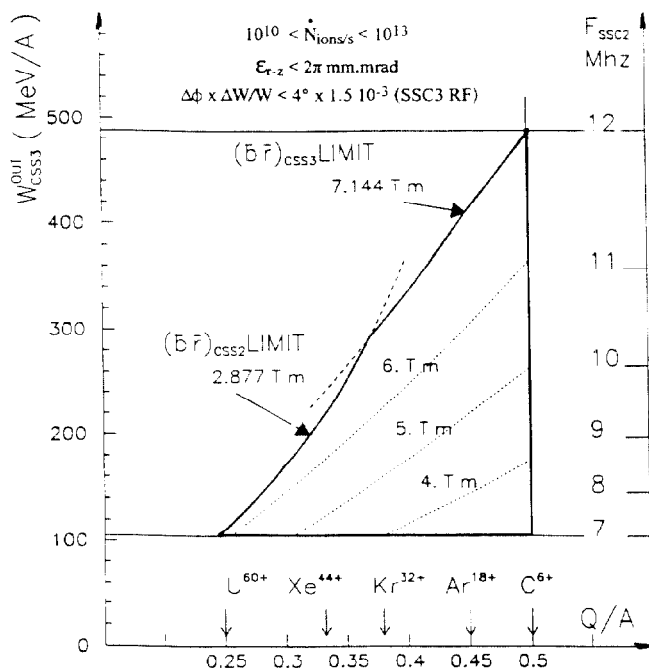


Figure 1 : SSC3 energy range versus  $Q/A$ .

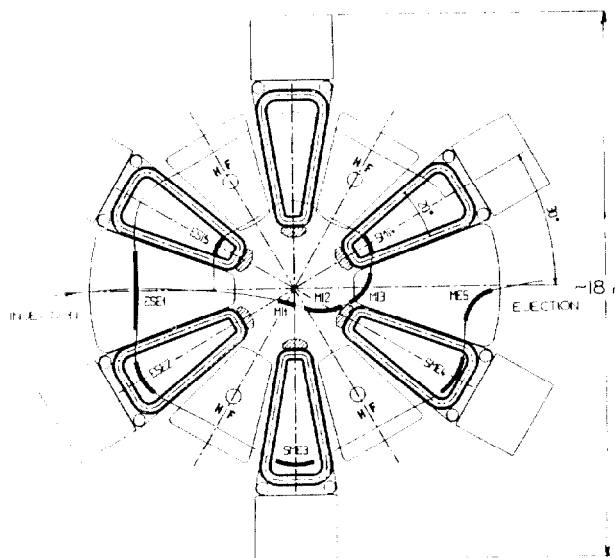


Figure 2 : Sketch of SSC3 including injection and injection elements.

Synchronism between the two cyclotrons SSC3 and SSC2 implies  $\bar{r}_{in} = 1.5 h/k (f_{SSC3} = k f_{SSC2})$ . In order to keep  $\Delta\phi < 5^\circ$  (rebuncher size),  $k$  is restricted to values  $\leq 4$  and due to the efficiency of the double gap cavities we will use, the value of the harmonic has to be  $h \geq 4$ .

From these considerations it results  $\bar{r}_{in} \geq 1.5\text{ m}$  and a moderate averaged maximum field  $\bar{B} \leq 2.4\text{ T}$  favouring a totally separated sector magnet using superconducting coils around each pole. Such a solution was first studied at Munich.

Due to the enhancement of the field flutter from the separated superconducting coils,  $v_z$  is increased as compared to the well known hard-edge results so that a 6 radial sector geometry seems appropriate up to 500 MeV/A.

In such a geometry it is possible to place 4 cavities and so to approach the turn separation required for a single turn extraction. In a first design we had chosen  $\bar{r}_{in} = 1.875\text{ m}$  and sectors of  $26^\circ$  but it turns out that injection and extraction were difficult and that we had to cross  $v_z = 1$ . A new set of parameters was then worked out to eliminate these problems; the main ones are given in table 1 and a sketch of the machine displayed on figure 2.

6 sectors	: $19.6^\circ$ between radial axes of the coils.
mean radii (m)	: $\bar{r}_{in} = 2.5$ ; $\bar{r}_{out} = 5.0$ .
mean field at ejection (T)	: $1.429 \geq \bar{B}_{out} \geq 0.609$ .
mean field increase (%)	: $8.6 \leq \bar{B}_{out}/\bar{B}_{in} \leq 41$ .
4 RF double gap cavities	: $\approx 30^\circ$ between gap axes.
Frequency range	: 21 - 36 MHz on harmonic $h = 5$ .
Maximum voltage at 36 MHz	: 500 kV ( $\leq 160\text{ kW}$ ).

Table 1 : SSC3 main parameters.

## II. Magnetic structure.

Due to the large range of energy and ion species, the required field laws are very different and for the most difficult operating point, the induction in the sector between the injection and ejection radii raises by more than one Tesla. As a consequence, correction coils must provide a high field value and one peculiarity of the machine will be to work with superconducting trim coils.

A sector magnet has been designed according to the following main options as shown on figure 3 :

- room-temperature poles with a large yoke to reduce the stray-fields,
- main coil and superconducting trim coils related to one pole enclosed in the same cryostat, its vacuum tank being closed by the magnet circuit,
- direct mechanical link between the upper and lower main coils, through their cryostats,
- a separated vacuum chamber with 15 cm axial clearance to accommodate the injection and ejection elements,
- a set of warm conductors, located between the beam and the cryostat vacuum chambers to provide the necessary small adjustments of the field pattern.

A preliminary technological study of the cryogenic parts (coils and cryostat) has been performed in Saclay (Service des Techniques Instrumentales des Particules Élémentaires).

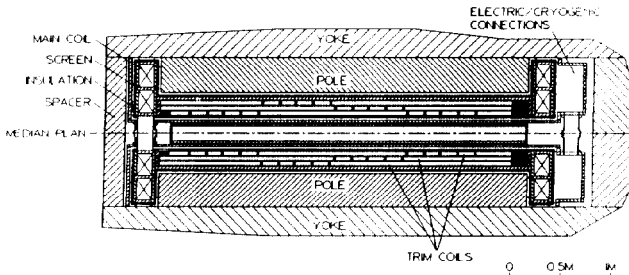


Figure 3 : Layout of the sector structure.

**II.1. Main coils :** We have chosen hollow conductors cooled by a forced flow of supercritical He so that a classical impregnated winding, more favourable than the bath system to hold the forces could be used. The overall maximum current density of  $45 \text{ A/mm}^2$  is below the technological limits but was chosen for stability and protection reasons.

The magnetic forces, calculated with TOSCA, tend to make the coil circular and the strongest component integrated along the straight side reaches  $12000 \text{ N}$  as shown on figure 4.

The coil is placed inside a thick stainless steel box divided into two parts for strengthening and all along and between the straight sides of this box, a plate gives a maximum stiffness.

Computed mechanical behaviour with such a structure gives a maximum radial deformation of 3 mm. The tolerances haven't been studied yet. It will be necessary to find the field perturbations introduced by the geometrical defects and to determine their influence on the beam behaviour.

**II.2 Correction coils :** These coils are located inside the main coils, in three layers. In spite of a lower efficiency (smaller magnetic angle) this configuration is chosen in order to get the main coils as close as possible to the median plane.

The conductors are distributed according to the field

variation law. This method is very attractive, minimizing the number of currents whose connexions require a lot of room. With only three independant currents we managed to fulfill the requested field pattern for any field level and energy. The residual corrections to be applied are small enough to be obtained with classical warm trim coils.

If necessary, a set of "nose" conductors could be added to compensate for both the negative return flux produced by the trim coils and the natural main field fall off.

Weight (iron only)	500 t
Stored energy - main coil	50 MJ
- trim coils	25 MJ
<b>Main coil (one coil)</b>	
Ampere turns	$< 3 \cdot 10^6 \text{ A}$
Max intensity	12000 A
Overall current density	$< 46 \text{ A/mm}^2$
12 double pancakes of $2 \times 10$ turns ( $150 \times 420 \text{ mm}^2$ )	240 turns
Proposed conductor : 54 wires Cu-NbTi. Diameter 1 mm - Cu/Sc = 1.3 - around a rectangular tube $12.2 \times 14.3 \text{ mm}^2$ , cooling channel $\phi = 7 \text{ mm}$ .	
<b>Trim coils (one set)</b>	
Ampere turns	$6 \cdot 10^5 \text{ A}$
Max intensity	2500 A
Overall current density	$25 \text{ A/mm}^2$
3 layers of 10 conductors ( $20 \times 40 \text{ mm}^2$ ) each one made of 8 elementary conductors	240 turns
Proposed conductor : 14 wires (same type as for main coils) inside an Al stabilizer of $5 \times 20 \text{ mm}^2$ .	

Table 2 : Main characteristics of a sector magnet.

**II.3. Field calculations :** The field calculations are performed using the 3D code TOSCA. The 6 sectors are always introduced, their mutual influence being very important.

Exemples of the results are displayed on figures 4, 5, 6 which show clearly the characteristics of this magnetic structure : main field patterns, trim-coil contributions, isochronous field laws obtained. We can notice the reverse field outside the loops of the cryogenic coils and the isochronous field laws obtained which are within some tens of gauss from the theoretical ones (average field along the trajectories). This residual  $\delta \vec{B}(\vec{r})$  shown on figure 7 can be reduced to the required level of some gauss using the warm trim coils.

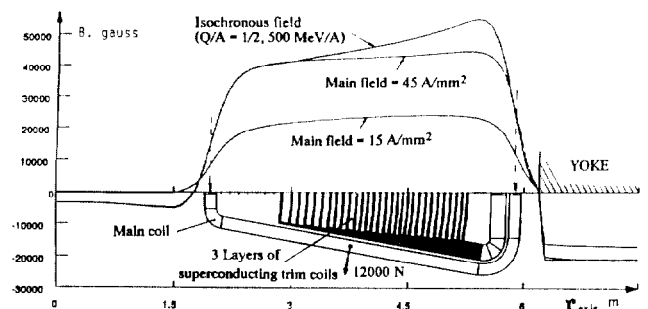


Figure 4 : Field along the sector axis and cryogenic trim coil setting on the 3 layers.

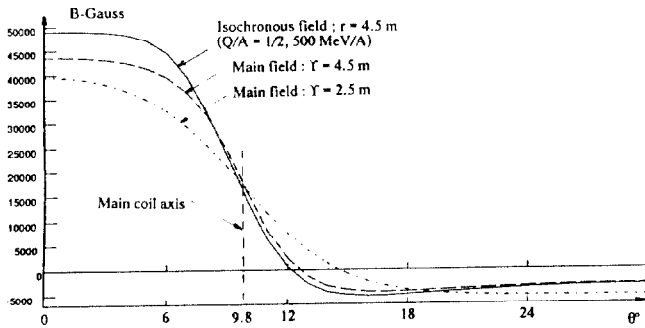


Figure 5 : Field at given radii from a sector axis to a valley axis.

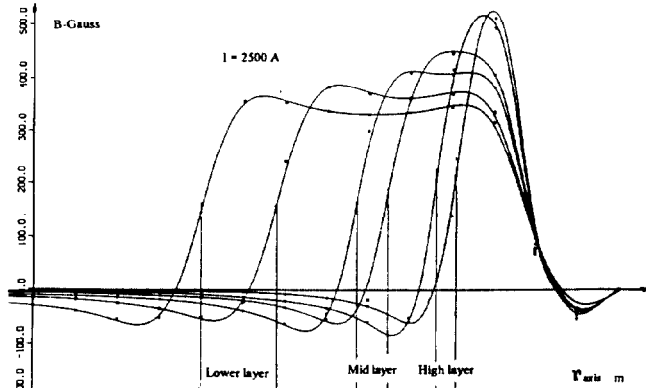


Figure 6 : Field added by a trim coil along a sector axis.

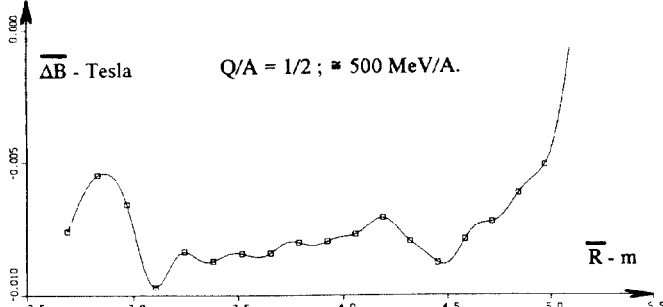


Figure 7 : Residual mean field error versus mean radius.

II.4.  $v_r v_z$  curves : These curves are shown for the extreme cases on the figure 8 ; the hard edge results are also displayed for comparison. The high  $v_z$  obtained are typical of the high flutter given by the superconducting coils : in such a geometry we can use straight poles at least up to  $\approx 500$  MeV/A.

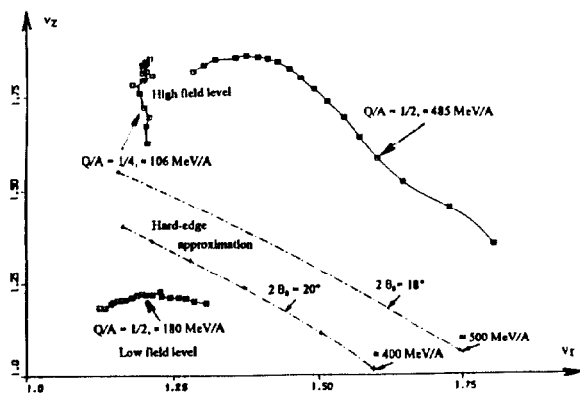


Figure 8 :  $v_r v_z$  curves in SSC3.

### III. Accelerating cavities.

We have chosen double gap cavities well adapted to the frequency range and able to sustain high voltages. The main tuning is provided by sliding short circuits, capacitive pannels being excluded at these voltage levels. The first calculations show no major problem to fulfill our requirements. A sketch of such a cavity is shown on figure 9.

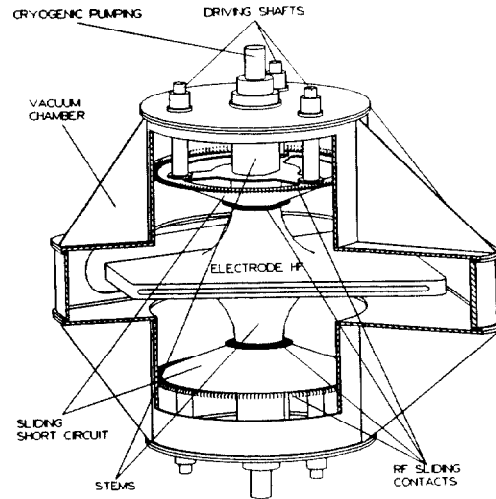


Figure 9 : Sketch of an accelerating cavity.

### IV. Injection and ejection systems.

The use of 4 double gap cavities able to sustain 500kV and the large  $\bar{r}_{in}$ ,  $\bar{r}_{out}$  of the machine account for a rather large turn spacing. Nevertheless we have to use a precession effect in order to get enough turn separation for a single turn extraction.

The characteristics of the elements shown on figure 2 are given in table 3. Most of these elements must be movable (some cm), both in injection and ejection systems.

<u>Injection</u>	1 Superconducting Magnet	2.5 T
	2 Superconducting Magnet	2.5 T
	3 Superconducting Septum Magnet	1 T
	4 Magnetic Septum	0.25 T
	5 Electrostatic Septum	60 kV/cm
<u>Ejection</u>	1 Electrostatic Septum	70 kV/cm
	2 Electrostatic Septum	60 kV/cm
	3 Magnetic Septum	- 0.3 T
	4 Magnetic Septum	- 1 T
	5 Superconducting Magnet	$B \rho \leq 7.2 \text{ Tm}$

Table 3 : Characteristics of injection and ejection elements.

### V. Conclusion.

Our preliminary studies led us to the solution here exposed. Many detailed design questions and technological problems will have to be solved and the tolerances have to be determined. Anyway the feasibility of such a machine seems rather well established.